第 48 卷 第 5 期/2021 年 3 月/中国激光 研究论文

中国激光

小型化宽调谐 MgO：PPLN 中红外纳秒光参量振荡器

王菲菲[1]，聂鸿坤[1]，刘俊亭[1]，杨克建[1,2]，张百涛[1,2*]，何京良[1,2]

[1]山东大学晶体材料国家重点实验室，新一代半导体材料研究院，山东 济南 250100；

[2]山东大学激光与红外系统集成技术教育部重点实验室，山东 青岛 266237

摘要 基于光学超晶格的光参量振荡技术是产生 2～5 μm 中红外光源的有效途径，在大气环境监测、医疗诊断、精密光谱分析、光电对抗等领域具有重要的应用价值。针对小型化中红外激光器应用需求，开展了结构紧凑、高效率、宽调谐的纳秒光纤激光泵浦的周期极化掺镁铌酸锂光学超晶格（MgO：PPLN）光参量振荡器（OPO）的研究。采用 1.06 μm 纳秒光纤激光泵浦多周期（29～31.6 μm）MgO：PPLN 晶体，结合周期和温度调谐，实现了闲频光 2.37～4.01 μm 连续调谐中红外激光输出。当泵浦功率为 9.95 W 时，2.37～3.75 μm 平均输出功率均大于 1.7 W，其中 3.4 μm 平均输出功率最大，相应的功率和光光转化效率分别为 3.68 W 和 37%。重点讨论了在 2.4、2.7、3.8 和 4.0 μm 处的中红外激光输出特性，最大平均输出功率可分别达到 2.87、2.45、1.87 和 1.22 W，相应的光光转化效率分别为 17.2%、19.8%、11.2%和 8.6%。本文的研究结果为小型化宽调谐中红外激光器的研发提供了重要的实验依据。

关键词 激光器；中红外激光；光参量振荡器；MgO：PPLN 晶体；宽调谐

中图分类号 O437.7 **文献标志码** A **doi**：10.3788/CJL202148.0501015

1 引 言

中红外（MIR）激光在遥感探测、大气环境监测、医疗诊断、精密测量以及光电对抗等领域具有广阔的应用前景和不可替代的重要作用。2～5 μm 波段是大气的一个重要传输窗口，对大雾、烟尘等具有较强的穿透能力，在海平面上传输时受到气体分子吸收和悬浮物的散射小，被应用于自由空间光通信领域[1]；2.7 μm 中红外激光位于水分子的最强吸收带处，因而对人体组织的渗透性小，对周围组织的热损伤小，已广泛应用于生物医疗领域[2]；3～5 μm 波段对应多数气体分子的特征吸收峰，被称为“分子指纹区”，在微量气体探测领域有着广泛的民用价值，例如：油田开采、天然气管道泄漏探测，煤矿中甲烷气体探测以及有机污染源的监测等[3-5]。军事上红外制导导弹探测器的光谱响应范围在 3～5 μm 波段，针对红外导引头的光电对抗迫切需要该波段的激光光源[6-8]。另外，超强超短中红外波段激光可以产生高次谐波，实现高亮度、高对比度的阿秒光脉冲和中红外频率梳，也可作为光参量振荡器（OPO）泵浦源获得 5～8 μm 更长波长激光[9-10]。因此，鉴于 2～5 μm 中红外激光重要的应用背景和极大需求，它已成为国防和民用竞相研究开发的重点领域。

OPO 技术是目前获得 2～5 μm 中红外激光输出的最常用的技术手段[11]。利用 $ZnGeP_2$ 和 $AgGaS_2$ 等非线性晶体的 OPO 可以获得 3～5 μm 大功率中红外激光输出，但是这些晶体生长困难，并且它们对 2 μm 以下激光存在很强的吸收，不能使用成熟的 1 μm 波段激光泵浦。光学超晶格材料（如 PPLN）具有非线性系数大、调谐范围宽、调谐方式多样化和结构紧凑等优点，是高功率宽调谐中红

收稿日期：2020-11-03；**修回日期**：2020-11-27；**录用日期**：2020-12-14

基金项目：国家重点研发计划（2017YFB0405204）

*E-mail：btzhang@sdu.edu.cn

外激光器件的最佳选择。1995 年，Myers 等[12]采用 1064 nm Nd∶YAG 调 Q 脉冲激光作为泵浦源，首次实现了基于 PPLN 的 OPO，调谐范围 1.66～2.95 μm。从此之后，随着 PPLN、MgO∶PPLN、PPLT、PPKTP 等优良光学超晶格晶体的涌现，特别是二极管泵浦全固态激光器的迅猛发展，光学超晶格 OPO 取得了一系列突破性的进展[13-20]。传统的基于光学超晶格的 OPO 大多数采用半导体激光(LD)泵浦的全固态激光器作为泵浦源，随着光纤激光器的飞速发展，基于光纤激光器泵浦的光学超晶格 OPO 引起国内外研究学者的广泛关注。与全固态激光器相比，光纤激光器具有结构灵活紧凑、可靠性高、环境适用性好、光束质量好和成本低等优点，用于泵浦光学超晶格 OPO 易于实现激光器的小型化、模块化和集成化。2005 年，Chen 等[21]利用 50 W Yb 光纤激光器泵浦 MgO∶PPLN 晶体，采用四镜环形腔结构在室温下获得 10 W 的 2.9 μm 连续波中红外激光输出。2008 年，Vainio 等[22]报道了连续波 Yb 光纤激光器泵浦的 MgO∶PPLN OPO，获得瓦级 2.7～3.45 μm 中红外激光输出。2012 年，Lin 等[23]利用脉冲 Yb 光纤激光器泵浦 MgO∶PPLN 获得 5.5 W 的 3.82 μm 中红外激光输出。2014 年，Liu 等[24]采用纳秒 Yb 光纤激光器泵浦多周期 MgO∶PPLN 晶体实现了 1462～1645 nm 信号光和 3000～3900 nm 连续调谐中红外激光输出，在 3 μm 处得到最大平均输出功率 1.73 W，在 3.7 μm 处平均功率达到 1.03 W。2020 年，李博文等[25]采用全保偏光纤结构，基于被动全光同步的中红外差频技术，获得 2940～3260 nm 的皮秒脉冲激光输出，最大平均功率为 926 mW，峰值转换效率为 41%。

本文采用 1064 nm 纳秒光纤激光器作为泵浦源，多周期 MgO∶PPLN 为非线性晶体，采用单谐振 OPO 技术，结合晶体周期和温度调谐，实现了闲频光 2.37～4.01 μm 的宽调谐中红外激光输出。其中，2.37～3.75 μm 的平均输出功率均大于 1.7 W，并重点研究了 2.4、2.7、3.8、4.0 μm 处的中红外激光输出特性。

2 实验装置

实验装置如图 1 所示。泵浦源为 1064.2 nm 线偏振纳秒光纤激光器，最大输出功率为 20 W，脉宽为 200 ns，重复频率为 50 kHz，光束质量因子 M^2<1.1。泵浦光缩束后经 1/2 波片 A 后通过光隔离器，隔离器一方面能够有效防止返回的泵浦光损坏光纤激光器，同时与 1/2 波片组成可变光衰减器，可调节进入谐振腔的激光功率。透过的泵浦光束经 1/2 波片 B 之后将偏振方向调节为竖直方向，然后经焦距为 500 mm 的透镜聚焦之后入射到 OPO 谐振腔中，束腰位于 MgO∶PPLN 晶体的中心位置，直径约为 450 μm。实验测得入射到 OPO 谐振腔的最大泵浦功率为 16.7 W。采用的多周期 MgO∶PPLN 超晶格尺寸为 10 mm×1 mm×50 mm，极化周期从 29～31.6 μm，共 6 个周期(周期间隔为 0.5 μm，最后一个周期间隔 0.6 μm)，MgO 掺杂摩尔分数为 5%，晶体两端面未镀膜。MgO∶PPLN 晶体放置在自制温控炉中，温控范围 20～200 ℃，温控精度为±0.1 ℃。M1 和 M2 构成平-平 OPO 谐振腔，腔长为 53 mm。为提高转换效率和输出激光光谱及功率稳定性，选用双通单谐振 OPO 结构，由于调谐范围较宽，需要两套镀膜参数不同的谐振腔镜，具体腔镜镀膜参数如表 1 所示，其中，HR 表示高反射，HT 表示高透过。

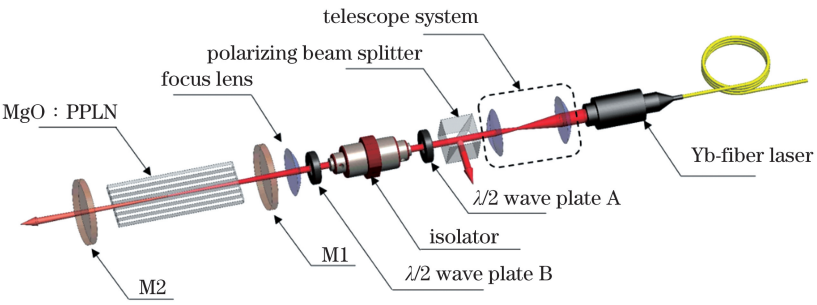

图 1 纳秒光纤激光器泵浦中红外 OPO 实验装置图

Fig. 1 Experimental setup of MIR OPO pumped by a nanosecond fiber laser

表 1 OPO 腔镜镀膜参数

Table 1 OPO cavity mirror coating parameters

OPO cavity mirror	Period Λ=29–31 μm	Period Λ=31.6 μm
M1	HT@1.06 μm; HR@1.4–1.6 μm, 3.29–3.9 μm	HT@1.06 μm; HR@1.7–2.0 μm, 2.4–2.9 μm
M2	HR@1.06 μm, 1.4–1.6 μm; HT@3.29–3.9 μm	HR@1.06 μm, 1.7–2.0 μm; HT@2.4–2.9 μm

3 实验结果与分析

首先对 OPO 所能得到的最长和最短波长进行了研究。当 MgO∶PPLN 的周期为 29 μm 时，温度控制在 40 ℃，调节入射泵浦光功率和谐振腔镜，在泵浦功率为 3.9 W 时 OPO 起振。此时，用光谱仪测得的输出信号光光谱如图 2(a)所示，中心波长为 1449.0 nm。根据能量守恒：$\lambda_p^{-1}=\lambda_s^{-1}+\lambda_i^{-1}$（式中：$\lambda_p$ 为泵浦光波长；λ_s 为信号光波长；λ_i 为闲频光波长），可知对应的最长闲频光波长为 4014.4 nm。同样，当 MgO∶PPLN 周期为 31.6 μm 时，温度控制在 180 ℃，此时 OPO 的振荡阈值为 1.1 W，用光谱仪测得的输出信号光光谱如图 2(b) 所示，中心波长为 1932.6 nm，对应的最短闲频光波长为 2370.8 nm。进一步，通过对 29～31.6 μm 共 6 周期的 MgO∶PPLN 晶体进行周期和温度调谐，实现了闲频光 2370.8～4014.4 nm 连续宽调谐纳秒中红外激光输出，调谐宽度为 1643.6 nm，波长调谐曲线如图 2(c)所示。其中温度调谐范围为 40～180 ℃，相邻周期的输出波长范围有部分重叠。

考虑光学超晶格的周期和温度，利用三波耦合方程对其调谐波长与温度和周期的关系进行了理论模拟。在 OPO 过程中，三波需要满足能量守恒和动量守恒。其中，能量守恒满足

$$\frac{1}{\lambda_p}=\frac{1}{\lambda_s}+\frac{1}{\lambda_i}。\tag{1}$$

动量守恒满足

$$\frac{n_p(\lambda_p,t)}{\lambda_p}-\frac{n_s(\lambda_s,t)}{\lambda_s}-\frac{n_i(\lambda_i,t)}{\lambda_i}-\frac{1}{\Lambda}=0,\tag{2}$$

式中：n_p、n_s 和 n_i 分别是泵浦光、信号光和闲频光折射率，折射率是温度 t 和波长 λ 的函数。MgO∶PPLN 晶体(MgO 掺杂摩尔分数为 5%)的 e 光折射率 Sellmeier 方程为

$$n_e^2(\lambda,t)=a_1+b_1f+\frac{a_2+b_2f}{\lambda^2-(a_3+b_3f)^2}+\frac{a_4+b_4f}{\lambda^2-a_5^2}-a_6\lambda^2。\tag{3}$$

(3)式中各参数值如表 2 所示。其中，f 是温度 t 的函数，表示为

$$f=(t-24.5)(t+570.82)。\tag{4}$$

(1)～(4)式理论模拟的结果如图 2(c)实线所示，从图中可以看出，实验中得到的波长随温度和周期的变化与理论计算结果符合较好。近几年，国内

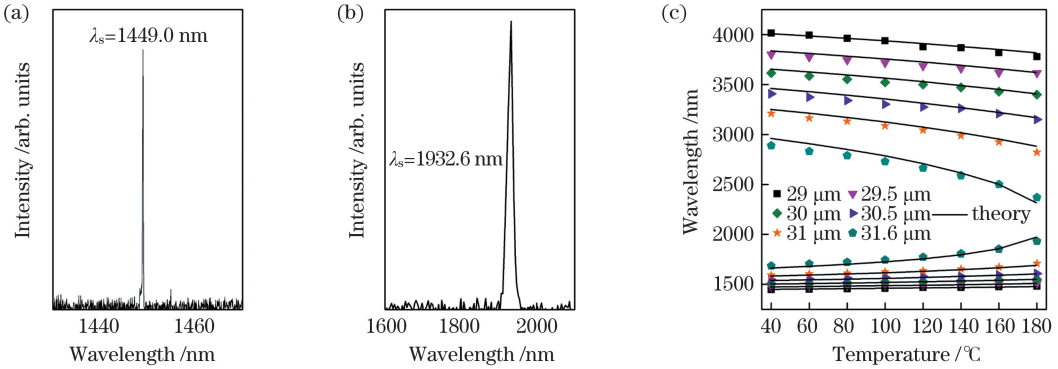

图 2 MgO∶PPLN OPO 波长调谐范围。(a) 29 μm 周期，温度 40 ℃时信号光光谱图；(b) 31.6 μm 周期，温度 180 ℃时信号光光谱图；(c)波长调谐范围

Fig. 2 Wavelength tunable capability of MgO∶PPLN OPO. (a) Signal light spectrum of 29 μm period at 40 ℃; (b) signal light spectrum of 31.6 μm period at 180 ℃; (c) wavelength tunable range

外利用光纤激光泵浦 PPLN 中红外 OPO 的代表性工作如表 3 所示，同时把本文的研究结果列于表中以便比较。相比而言，本文利用纳秒 Yb 光纤激光器泵浦 6 周期 PPLN 超晶格得到了更宽的中红外调谐范围(2370.8～4014.4 nm)，同时具有更高的泵浦光-参量光转化效率(37.0%@3.4 μm)。

表 2 Sellmeier 方程中的各参数值

Table 2 Parameter values in Sellmeier equation

Parameter	Value	Parameter	Value
a_1	5.756	a_6	0.0132
a_2	0.0983	b_1	2.86×10^{-6}
a_3	0.202	b_2	4.7×10^{-8}
a_4	189.32	b_3	6.113×10^{-8}
a_5	12.52	b_4	1.516×10^{-4}

表 3 光纤激光器泵浦中红外 PPLN OPO 研究进展

Table 3 Research progresses of MIR PPLN OPO pumped by fiber laser

Pump source parameter	Crystal parameter	MIR laser output characteristic	Reference
Yb fiber laser@1064 nm, 20 W, 81.1 MHz	MgO∶PPLN, 50 mm, 28.5–30.5 μm period	3.06–4.16 μm, 4.6 W@3.33 μm, optical-optical efficiency 28.7%	[26]
Yb fiber optic amplifier, 10 W	MgO∶PPLN, 40 mm, 29.98 μm period	0.9 W@2900 nm, M^2～1.1	[27]
Yb fiber laser @1064 nm, 20 W, 20 ps, 80 MHz	MgO∶PPLN, 50 mm, 30.5 μm period	3118–3393 nm, 290 mW@3393 nm, optical-optical efficiency ～3.8%	[28]
Yb fiber laser @1064 nm, 20 W	MgO∶PPLN, 50 mm, 28.5–31.5 μm, 6 period	3.0–3.9 μm, 1.73 W@3.0 μm, 1.03 W@3.7 μm	[24]
Yb fiber laser @1064 nm, 20 W, 20 ps, 9.4 MHz	MgO∶PPLN, 35 mm, 28 μm period, angle from 0°–30°	2418–4307 nm, 1.7 W@2950 nm	[29]
Nanosecond Yb/Er fiber optic amplifier @1065 nm, 29 W	MgO∶PPLN, 40 mm, 29.98 μm period	3.31–3.48 nm, 6 W@3.35 μm, M^2～1.4	[30]
Yb fiber laser @1064 nm, 14 W	MgO∶PPLN, 40 mm; 29.52–31.59 μm period	2260–3573 nm, 2.4 W@2991.5 nm (peak power～30 W);	[31]
Yb fiber laser @1064 nm, 20 W	MgO∶PPLN, 50 mm, 29–31.6 μm, 6 period	2370.8–4014.4 nm, 3.68 W@3.4 μm	Proposed

为了防止超晶格材料被打坏，实验中固定泵浦功率为 9.95 W，改变 MgO∶PPLN 超晶格周期和温度，得到闲频光平均输出功率随波长的变化散点图，如图 3(a)所示。从图中可以看出，2370.8～3750.0 nm

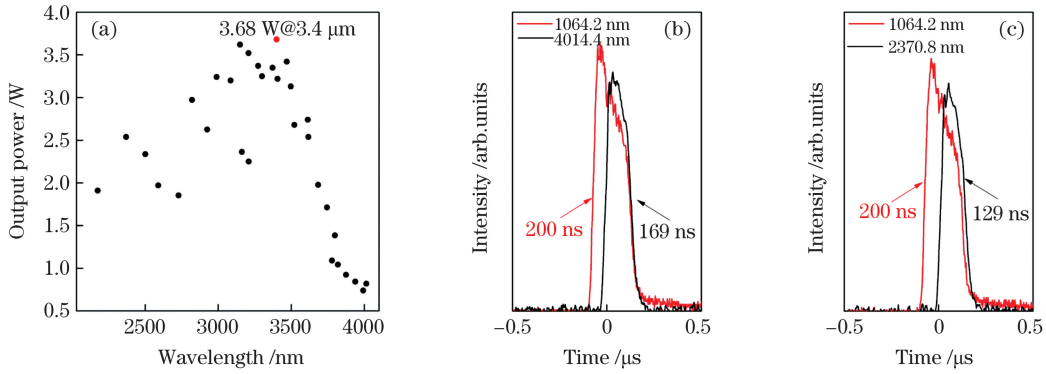

图 3 泵浦功率为 9.95 W 时激光输出特性。(a)闲频光平均输出功率随波长的变化；(b) 4014.4 nm 和残余 1064.2 nm 脉冲波形；(c) 2370.8 nm 和残余 1064.2 nm 脉冲波形

Fig. 3 Laser output characteristics at 9.95 W pump power. (a) Average output power at different wavelength; (b) pulse profile at 4014.4 nm and residual 1064.2 nm; (c) pulse profile at 2370.8 nm and residual 1064.2 nm

平均功率均大于 1.7 W，相应的转化效率大于 17.1%。其中，波长为 3.4 μm 时，得到最大平均输出功率 3.68 W，对应的最大光光转化效率 37.0%。采用 HgCdTe 光电探测器和示波器（1 GHz，DPO 7102，Tektronix，USA）对 4014.4 nm、2370.8 nm 和残余泵浦光同步输出的时域脉冲波形进行了测量，分别如图 3(b)和(c)所示，从图中可以看出，泵浦光脉冲顶部被消耗掉一部分转变为参量光脉冲输出。4014.4 nm 和 2370.8 nm 脉冲宽度分别为 169 ns 和 129 ns。

另外，对 2.4、2.7、3.8、4.0 μm 波长处的 OPO 输出特性进行了探究。图 4 给出了这四个波长对应的平均输出功率随泵浦功率的变化曲线，从图中可以看出，2.4、2.7、3.8、4.0 μm 的振荡阈值分别为 1.10、1.41、3.25、3.90 W，最大平均输出功率分别为 2.87、2.45、1.87、1.22 W，相应的光光转换效率分别为17.2%、19.8%、11.2%、8.6%。在最高输出功率处对应的脉冲宽度分别为 129、132、159、169 ns，对应的单脉冲能量分别为 57.4、49.0、37.4、24.4 μJ，相应参数如表 4 所示。

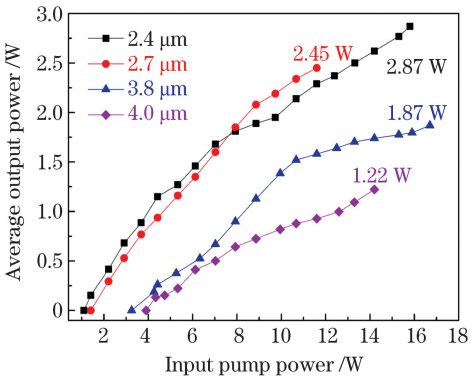

图 4　2.4、2.7、3.8、4.0 μm 平均输出功率随泵浦功率变化曲线

Fig. 4　2.4, 2.7, 3.8, and 4.0 μm average output power variation curves with pump power

表 4　2.4、2.7、3.8、4.0 μm 输出功率分析

Table 4　2.4, 2.7, 3.8, and 4.0 μm output power analysis

Wavelength /μm	Input power /W	Maximum output power /W	Optical-optical efficiency /%	Single pulse energy /μJ	Peak power /W
2.4	16.7	2.87	17.2	57.4	445.0
2.7	12.4	2.45	19.8	49.0	371.2
3.8	16.7	1.87	11.2	37.4	235.2
4.0	14.2	1.22	8.6	24.4	144.4

利用光束质量分析仪（NanoScan by PHOTOH，Inc.）对 2.4、2.7、3.8、4.0 μm 的闲频光进行了光束质量分析。四个波长分别在最高功率下测量的光束质量因子 M^2，结果如图 5 所示，插图为对应波长下二维和三维光斑图。从实验结果来看，在高功率下，输出激光的光斑产生了一定的畸变。此外，对四个波长在最高平均输出功率下的功率稳定性进行了测试，测试结果如图 6 所示，2 h 不稳定性均方根（RMS）分别为 2.51%、2.24%、2.35%、2.60%。

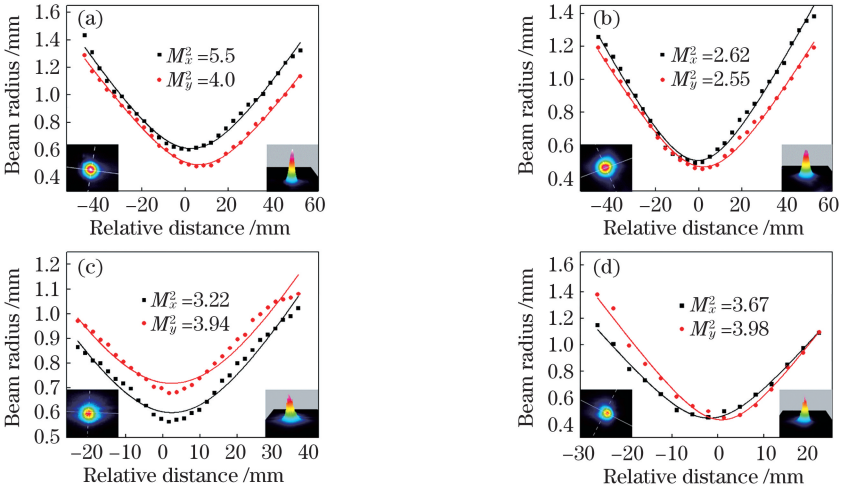

图 5　最高功率下光束质量。(a) 2.4 μm；(b) 2.7 μm；(c) 3.8 μm；(d) 4.0 μm

Fig. 5　Beam quality at maximum power. (a) 2.4 μm; (b) 2.7 μm; (c)3.8 μm; (d)4.0 μm

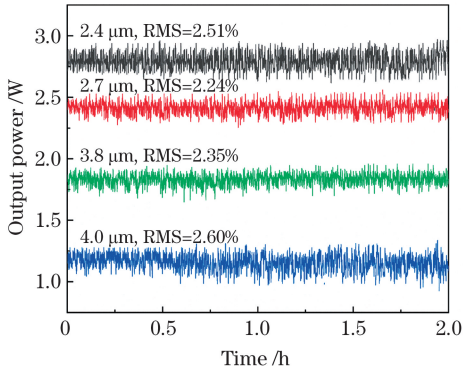

图 6 2.4、2.7、3.8、4.0 μm 最高平均功率下稳定性

Fig. 6 Stability at maximum average power of 2.4, 2.7, 3.8, and 4.0 μm

4 结 论

本文设计了一种小型化宽调谐纳秒中红外光参量振荡器。采用中心波长为 1064.2 nm 的纳秒光纤激光器泵浦 29～31.6 μm 共计 6 周期的 MgO∶PPLN 晶体，通过改变晶体周期并在 40～180 ℃进行连续的温度调谐，实现了闲频光 2370.8～4014.4 nm 连续调谐输出，调谐宽度为 1643.6 nm。在输入功率为 9.95 W 时，2370.8～3750.0 nm 的平均输出功率均大于 1.7 W。其中，在 3.4 μm 处得到最大平均功率 3.68 W，对应的泵浦光-参量光转化效率达到 37.0%。当闲频光输出波长分别为 2.4、2.7、3.8、4.0 μm 时，得到最大平均输出功率分别为 2.87、2.45、1.87、1.22 W，相应的光光转化效率分别为 17.2%、19.8%、11.2%、8.6%，对应的单脉冲能量分别为 57.4、49.0、37.4、24.4 μJ。MgO∶PPLN 晶体在 4 μm 左右吸收增加，闲频光输出功率逐渐变小。本文的研究结果为小型化宽调谐中红外激光光源的研发提供了实验依据。

参 考 文 献

[1] Zhang Z, Su L B. Research progress of near 3 μm mid-infrared laser based on Er^{3+} doped single crystals [J]. Journal of Synthetic Crystals, 2020, 49(8): 1361-1368.
张振, 苏良碧. 掺 Er^{3+} 晶体近 3 μm 中红外激光研究进展[J]. 人工晶体学报, 2020, 49(8): 1361-1368.

[2] Frauchiger J, Lüthy W. Interaction of 3 μm radiation with matter[J]. Optical and Quantum Electronics, 1987, 19(4): 231-236.

[3] Geiser P, Wilier U, Schade W. Picosecond mid-infrared LIDAR system [C] // 2005 Quantum Electronics and Laser Science Conference, May 22-27, 2005, Baltimore, MD, USA. New York: IEEE Press, 2005: 1986-1987.

[4] Weibring P, Edner H, Svanberg S. Versatile mobile lidar system for environmental monitoring [J]. Applied Optics, 2003, 42(18): 3583-3594.

[5] Tan G J, Xie J J, Zhang L M, et al. Recent progress in mid-infrared laser technology[J]. Chinese Optics, 2013, 6(4): 501-512.
谭改娟, 谢冀江, 张来明, 等. 中波红外激光技术最新进展[J]. 中国光学, 2013, 6(4): 501-512.

[6] Hecht J. History of gas lasers, part 1-continuous wave gas lasers [J]. Optics and Photonics News, 2010, 21(1): 16.

[7] Hudson R D. Infrared system engineering [M]. New York: Wiley, 1969: 102-103.

[8] Zhong M, Ren G. 3–5 μm medium infrared laser countermeasure weapon system [J]. Sichuan Ordnance Journal, 2007, 28(1):3-6.
钟鸣, 任钢. 3～5 μm 中红外激光对抗武器系统[J]. 四川兵工学报, 2007, 28(1):3-6.

[9] Vodopyanov K L, Schunemann P G. Broadly tunable noncritically phase-matched $ZnGeP_2$ optical parametric oscillator with a 2 μJ pump threshold[J]. Optics Letters, 2003, 28(6): 441-443.

[10] Qian C P, Shen Y J, Yao B Q, et al. High power far-infrared ZGP OPO laser[C]//2016 Conference on Lasers and Electro-Optics (CLEO), June 5-10, 2016, San Jose, CA, USA. New York: IEEE Press, 2016: 1-2.

[11] Ren G. Studies on the mid-infrared optical parametric oscillators and their applications [D]. Chengdu: Sichuan University, 2006: 28-36.
任钢. 中红外光参量振荡器及其应用技术的研究[D]. 成都: 四川大学, 2006: 28-36.

[12] Myers L E, Miller G D, Eckardt R C, et al. Quasi-phase-matched 1.064-microm-pumped optical parametric oscillator in bulk periodically poled $LiNbO_3$[J]. Optics Letters, 1995, 20(1): 52-54.

[13] Elder I, Legge D, Beedell J, et al. Nd∶YVO_4 pumped degenerate PPLN OPO[C]//Advanced Solid-State Photonics, Incline Village, Nevada. Washington, D.C.: OSA, 2006.

[14] Peng Y F, Wei X B, Luo X W, et al. High-power and widely tunable mid-infrared optical parametric amplification based on PPMgLN[J]. Optics Letters, 2016, 41(1): 49-51.

[15] Lai C M, Hu I N, Lai Y Y, et al. Upconversion blue laser by intracavity frequency self-doubling of periodically poled lithium tantalate parametric oscillator[J]. Optics Letters, 2010, 35(2): 160-162.

[16] Jeong Y C, Hong K H, Kim Y H. Bright source of

polarization-entangled photons using a PPKTP pumped by a broadband multi-mode diode laser[J]. Optics Express, 2016, 24(2): 1165-1174.

[17] Chuchumishev D, Marchev G, Buchvarov I, et al. Sub-ns OPO based on PPKTP with 1 mJ idler energy at 2.8 μm[C]//2013 Conference on Lasers & Electro-Optics Europe & International Quantum Electronics Conference CLEO EUROPE/IQEC, May 12-16, 2013, Munich, Germany. New York: IEEE Press, 2013: 1.

[18] Wang Y H, Liu H Y, Wang Z Y, et al. 4.1 μm high power mid-infrared intra-cavity optical parametric oscillator[J]. Acta Photonica Sinica, 2019, 48(8): 0823002.
王宇恒, 刘贺言, 王泽宇, 等. 4.1 μm 高功率中红外内腔光参量振荡器[J]. 光子学报, 2019, 48(8): 0823002.

[19] Li H N, Zhang D C, Zhu J F, et al. Nanosecond mid-infrared tunable parametric laser [J]. Acta Optica Sinica, 2019, 39(11): 1114002.
李浩宁, 张大成, 朱江峰, 等. 纳秒中红外可调谐参量激光研究[J]. 光学学报, 2019, 39(11): 1114002.

[20] Hu X L, Gan J W, Yang Z J, et al. Difference-frequency generation of mid-infrared picosecond laser by pulse synchronization technology based on all polarization-maintaining fibers [J]. Acta Optica Sinica, 2020, 40(7): 0736001.
胡晓蕾, 甘继伟, 杨占军, 等. 基于全保偏光纤利用脉冲同步技术差频产生中红外皮秒激光[J]. 光学学报, 2020, 40(7): 0736001.

[21] Chen D W, Rose T S. Low noise 10 W cw OPO generation near 3 μm with MgO doped PPLN[C]// Conference on Lasers and Electro-Optics /Quantum Electronics and Laser Science and Photonic Applications Systems Technologies, May 22-27, 2005, Baltimore, Maryland United States: CThQ2.

[22] Vainio M, Peltola J, Persijn S, et al. Singly resonant cw OPO with simple wavelength tuning[J]. Optics Express, 2008, 16(15): 11141-11146.

[23] Lin D J, Alam S U, Shen Y H, et al. Large aperture PPMgLN based high-power optical parametric oscillator at 3.8 μm pumped by a nanosecond linearly polarized fiber MOPA[J]. Optics Express, 2012, 20(14): 15008-15014.

[24] Liu S D, Wang Z W, Zhang B T, et al. Wildly tunable, high-efficiency MgO∶PPLN mid-IR optical parametric oscillator pumped by a Yb-fiber laser[J]. Chinese Physics Letters, 2014, 31(2): 024204.

[25] Li B W, Wu J M, Xu M H, et al. Research on passive synchronization based wide tuning medium infrared differential frequency technique[J]. Chinese Journal of Lasers, 2020, 47(11): 1115001.
李博文, 武佳美, 徐明航, 等. 基于被动同步的宽调谐中红外差频技术研究[J]. 中国激光, 2020, 47(11): 1115001.

[26] Kokabee O, Esteban-Martin A, Ebrahim-Zadeh M. Efficient, high-power, ytterbium-fiber-laser-pumped picosecond optical parametric oscillator[J]. Optics Letters, 2010, 35(19): 3210-3212.

[27] Hong X P, Shen X L, Gong M L, et al. Broadly tunable mode-hop-free mid-infrared light source with MgO∶PPLN continuous-wave optical parametric oscillator[J]. Optics Letters, 2012, 37(23): 4982-4984.

[28] Ramaiah-Badarla V, Chaitanya Kumar S, Ebrahim-Zadeh M. Fiber-laser-pumped, dual-wavelength, picosecond optical parametric oscillator[J]. Optics Letters, 2014, 39(9): 2739-2742.

[29] Chaitanya Kumar S, Wei J X, Debray J, et al. High-power, widely tunable, room-temperature picosecond optical parametric oscillator based on cylindrical 5% MgO∶PPLN[J]. Optics Letters, 2015, 40(16): 3897-3900.

[30] Murray R T, Runcorn T H, Guha S, et al. High average power parametric wavelength conversion at 3.31–3.48 μm in MgO∶PPLN[J]. Optics Express, 2017, 25(6): 6421-6430.

[31] Wu Y D, Liang S J, Fu Q, et al. Compact picosecond mid-IR PPLN OPO with controllable peak powers[J]. OSA Continuum, 2020, 3(10): 2741-2748.

Miniaturized Widely Tunable MgO∶PPLN Nanosecond Optical Parametric Oscillator

Wang Feifei[1], Nie Hongkun[1], Liu Junting[1], Yang Kejian[1, 2], Zhang Baitao[1, 2*], He Jingliang[1, 2]

[1] *State Key Laboratory of Crystal Materials, Institute of Novel Semiconductors, Shandong University, Jinan, Shandong* 250100, *China*;

[2] *Key Laboratory of Laser & Infrared System, Ministry of Education, Shandong University, Qingdao, Shandong* 266237, *China*

Abstract

Objective Mid-infrared (MIR) lasers play a role in several applications, including environmental atmosphere monitoring, medical diagnosis, spectral analysis, optoelectronic countermeasures, etc. The MIR band of wavelengths spanning 2–5 μm is called the atmospheric window area, which is the transmission window with the highest atmospheric transmittance. This band can penetrate fog and smoke and is widely used in the field of free space optical communication. A MIR laser with a wavelength near 3 μm is located in the most absorptive zone of water molecules. This laser has a shallow penetration depth in human tissues, leading to little thermal damage to surrounding tissues. This greatly improves the ability of the laser to melt, excise, and vaporize tissues; therefore, it is widely used in biomedical fields. The spectral response range of a military infrared guided missile detector is 3–5 μm. With the yearly increase of infrared detector usage, corresponding jamming technology development is also accelerating and a laser light source of this band is urgently needed for a photoelectric countermeasure of an infrared seeker. Motivated by the demand of miniaturized MIR laser sources, a compact, high-efficiency, and widely tunable magnesium-doped periodically poled lithium niobate (MgO∶PPLN) optical parametric oscillator (OPO) pumped by a nanosecond fiber laser was studied.

Methods Optical parametric oscillation with a superlattice is the most effective method for 2–5 μm MIR laser generation. The pump source in this study was a linearly polarized nanosecond fiber laser with a central wavelength of 1064.2 nm. The maximum output power of the pump was 20 W, the pulse width was 200 ns, the repetition frequency was 50 kHz, and the beam quality factor, M^2, was less than 1.1. A 1-mm-thick and 50-mm long MgO∶PPLN nonlinear crystal, with polarization periods of 29–31.6 μm, was used. We chose a double-pass single-resonance flat-flat cavity OPO and used the quasi-phase matching method to tune the wavelength by periodic and temperature modulation of the PPLN crystal. First, the period and temperature of the six-period MgO∶PPLN were continuously tuned and the wavelength tuning range realized by the OPO was explored. The relationship between the tuning wavelength and temperature and period was theoretically simulated using the three-wave coupling equation. The wavelength of the signal light was experimentally determined and then the three-wave coupling equation was used to calculate the corresponding wavelength of idle light. Then, the average idle light output power of different wavelengths was investigated. The output power at four particular wavelengths, 2.4, 2.7, 3.8, and 4.0 μm, was explored and analyzed. In addition, we used a beam quality analyzer (Nano Scan by PHOTOH, Inc.) to measure the beam quality of the wavelengths at the highest average output power. Finally, the power stability of each wavelength of interest, under the highest average output power, was tested.

Results and Discussions First, when the period of the MgO∶PPLN was 29 μm, the temperature was controlled at 40 ℃ and the OPO began oscillation when the incident pump light power was 3.9 W. At this time, the longest idle wavelength of the PPLN obtained was 4014.4 nm [Fig. 2(a)]. When the period of the MgO∶PPLN was 31.6 μm, the temperature was controlled at 180 ℃ and the shortest idle wavelength of the PPLN was 2370.8 nm [Fig. 2(b)]. Combined with periodic and temperature modulation, 2.37–4.01 μm widely tunable operation was realized with a multi-period (29–31.6 μm) MgO∶PPLN crystal [Fig. 2(c)]. In order to prevent damage to the superlattice material, the fixed pump power was 9.95 W. The period and temperature of MgO∶PPLN were changed to obtain a scatter diagram of the average idle light output power with wavelength [Fig. 3(a)]. The average output power of wavelengths ranging from 2370.8–3750.0 nm was greater than 1.7 W and the corresponding conversion efficiency

was greater than 17.1%. When the wavelength was 3.4 μm, the maximum average output power was 3.68 W and the corresponding maximum photoconversion efficiency was 37.0%. The wavelengths of 2.4, 2.7, 3.8, and 4.0 μm had maximum average power outputs of 2.87, 2.45, 1.87, and 1.22 W, respectively (Fig. 4), with corresponding optical conversion efficiencies of 17.2%, 19.8%, 11.2%, and 8.6%, respectively. At the highest output power, the corresponding pulse widths were 129, 132, 159, and 169 ns, and the corresponding single pulse energies were 57.4, 49.0, 37.4, and 24.4 μJ, for wavelengths of 2.4, 2.7, 3.8, and 4.0 μm, respectively (Table 4). The four wavelengths produced spot distortion at maximum power and the measured beam quality deteriorated (Fig. 5). In addition, the two-hour instability root mean square (RMS) of the four wavelengths at the highest average output power were 2.51%, 2.24%, 2.35%, and 2.60%, respectively (Fig. 6).

Conclusions A miniaturized wide-tuned infrared OPO with nanosecond pulse width was designed in this paper. A nanosecond fiber laser with a central wavelength of 1064.2 nm was used to pump 29–31.6 μm MgO∶PPLN crystals for six cycles. By changing the crystal period and continuously tuning the temperature at 40–80 ℃, the continuous tuning output of idle light at 2370.8–4014.4 nm with a tuning width of 1643.6 nm was realized. Under an incident pump power of 9.95 W, the average output powers were larger than 1.7 W for a wavelength range of 2.37–3.75 μm. The highest average output power of 3.68 W was obtained at 3.4 μm, corresponding to an optical-optical conversion efficiency of 37%. Moreover, the MIR OPO output parameters at 2.4, 2.7, 3.8, and 4.0 μm were investigated in detail. The maximum average output powers were determined to be 2.87, 2.45, 1.87, and 1.22 W with corresponding optical-optical conversion efficiencies of 17.2%, 19.8%, 11.2%, and 8.6%, respectively. Our results provide significant experimental basis for the development of miniaturized and widely tunable MIR laser sources.

Key words lasers; mid-infrared laser; optical parametric oscillator; MgO∶PPLN crystal; widely tunable

OCIS codes 140.3070; 190.4970; 160.3730; 140.3600